CHAPTER 4

THEORETICAL ANALYSIS OF HEAT PUMP DRYER

In this chapter, the details of the mathematical modeling and the simulation of the heat pump dryer represented the different low global warming potential (GWP) refrigerants (future refrigerants). The properties of the different refrigerants are provided in Table 4.1. The mathematical model of the heat pump dryer is divided into different sub-model such as the condenser model, compressor model, evaporator model, expansion device model, and the dryer model for an easy understanding of the simulation model. In each sub-model, the detailed calculation steps for the heat and the mass transfer are given. Various refrigerants are compared based on energetic and exergetic performance.

Table: 4.1. Properties of considered refrigerants

Refrigerant	Boiling point (°C)	Critical point (°C)	ODP	GWP	Flammability
R134a	-26.07	101.06	0	1300	No
R290	-42.1	96.7	0	20	Higher
R600	-0.7	152.01	0	4	Higher
R600a	-11.6	134.6	0	20	Higher
R152a	-24.1	113.3	0	140	Lower
R32	-51.7	78.1	0	650	Mild
R1234yf	-29.5	99.7	0	4	Mild
R1234ze(E)	-18.95	109.4	0	6	Mild

4.1. Modeling and simulation

The layout of the simulated batch type open cycle HPD consisting of the air-side working loop and the refrigerant-side working loop is shown in Fig. 4.1. T-s of the refrigerant loop and the psychrometric diagram for the air loop is shown in Figs. 4.2 and 4.3, respectively. The heat pump cycle works between the fixed evaporator temperature of 5°C and a condenser temperature of 40°C. Refrigerant enters the compressor in a superheated state at point 1 and leaves the compressor at point 2 in a superheated state. The superheated refrigerant coming from the compressor enters the condenser at state 2 and leaves the condenser at point 3 in the subcooled or two-phase region depending upon the air velocity and the inlet condition to the evaporator by dissipating heat to drying air. Refrigerant follows the isenthalpic expansion in the capillary tube (3-4) from the condenser pressure to the evaporator pressure. Then, the refrigerant enters the evaporator and leaves the evaporator at point 1 by absorbing heat from the air.

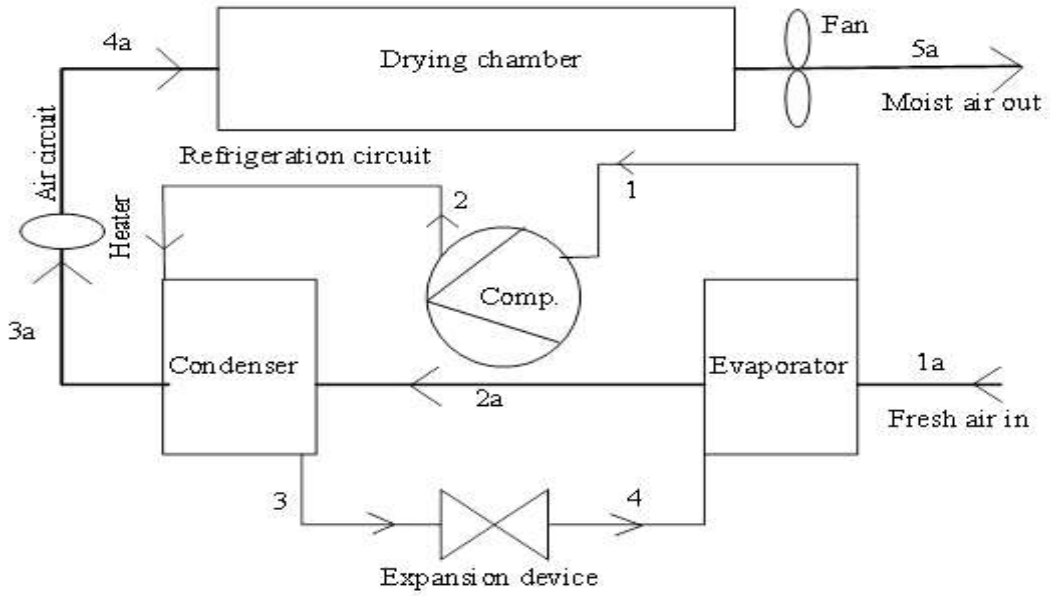

Fig. 4.1. Schematic diagram of open type HPD

The atmospheric air entering the evaporator at point 1a is dehumidified and cooled to a temperature below the dew point temperature and exits the evaporator at point

2a. Then the air enters the condenser at point 2a and sensible heating of air takes place and leaves the condenser at point 3a. A supplementary electric heater is used to heat the air to the desired temperature (process: 3a-4a). Hot and dry air enters the drying chamber at point 4a and extracts the moisture from the drying material while passing through the chamber and the air gets humidified and cooled and leaves the drying chamber at state 5a. In the drying chamber, it is considered that the air coming from the condenser is contacted with the drying material and there is no bypass of the air through the drying chamber.

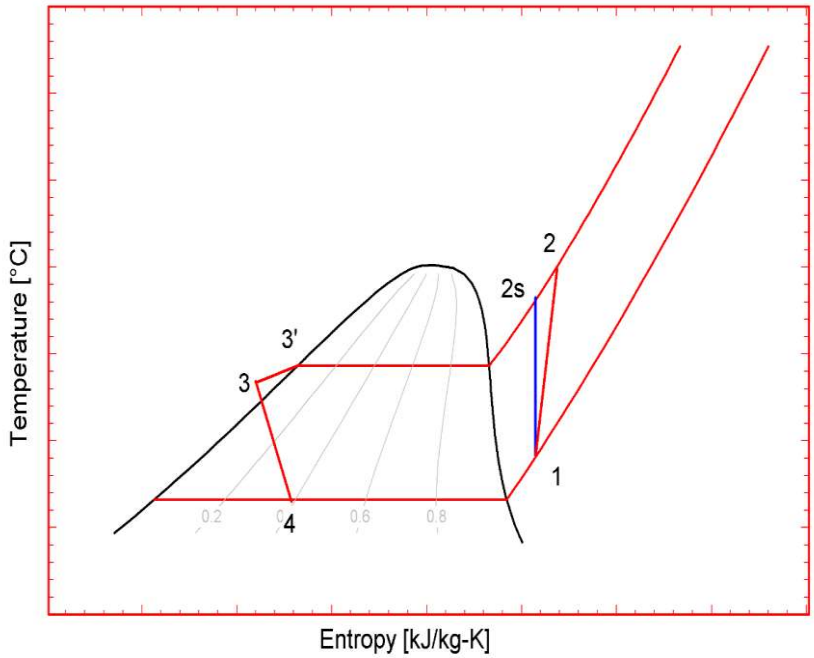

Fig. 4.2. Heat pump cycle on T-s diagram

The mathematical model of the considered HPD has been developed based on the energy and exergy balances of each component (compressor, evaporator, condenser, expansion device, fan, heater, and dryer). The following assumptions have been made for analysis:

- The steady-state operation of HPD is considered.
- The heat transfers of the component with ambient are negligible.

- The ambient conditions and specific heat of the air remain constant.
- The process of refrigerant in the compressor is adiabatic but not isentropic.
- The pressure drop of refrigerant in the different components is negligible.
- Conductive resistance of evaporator and condenser tubes is neglected.
- Air in the dryer follows the constant wet-bulb temperature line on the psychrometric chart.

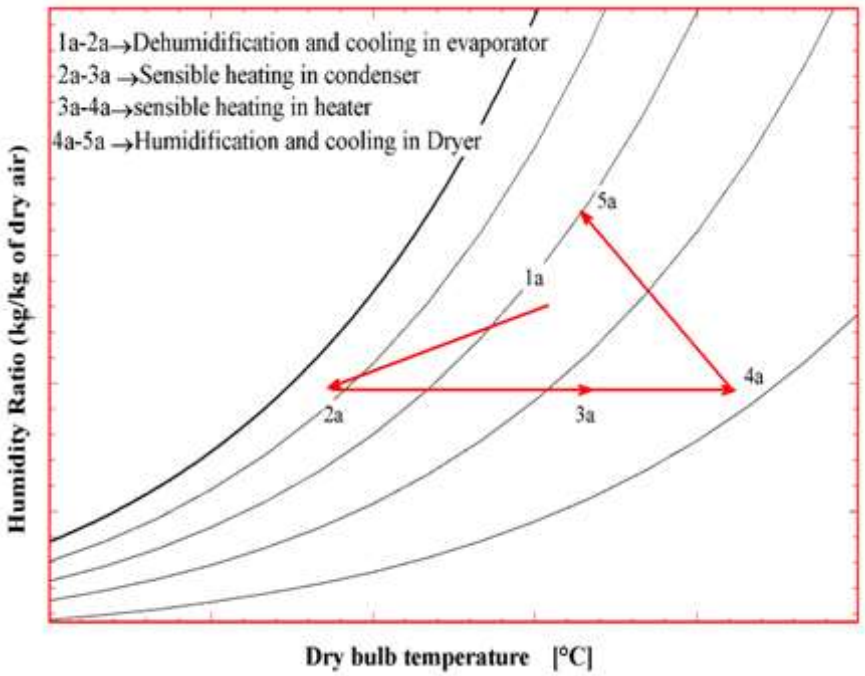

Fig. 4.3. Various processes on a psychrometric chart

4.1.1. Compressor model

Using the given specifications of the compressor, the mass flow rate of the refrigerant through the compressor has been calculated by,

$$\dot{m}_r = \rho_1 \eta_v V_s \left(N/60\right) \tag{4.1}$$

Then the enthalpy at the outlet of the compressor has been evaluated by,

$$h_2 = \frac{\left(h_{2s} - h_1\right)}{\eta_{isen}} + h_1 \tag{4.2}$$

Where volumetric and isentropic efficiencies of the compressor are given by (Bengtsson et al., 2014),

$$\eta_v = 1.04\left(1+0.1\frac{T_{evap}-18}{100}\right)\exp\left(-0.066\frac{p_{cond}}{p_{evap}}\right) \tag{4.3}$$

$$\eta_{isen} = \eta_v \Big/ \exp\left[-2.28\frac{T_{cond}+273}{T_{evap}+273}+2.67\right] \tag{4.4}$$

Then, the work done by the compressor has been calculated by,

$$\mathrm{W}_{comp} = \dot{m}_r\left(h_2 - h_1\right) \tag{4.5}$$

4.1.2. Condenser model

In the condenser, only heat is transferred from the refrigerant to air passing through the fin surface as there is no moisture transfer. The condenser used in this study is a wavy fin and tube cross-flow heat exchanger, which contains several rows and passes. It is considered that the mass flow rate of the air is equally divided in each pass. Total flow length has been divided into three zones for heat transfer calculation: sub-cooled, two-phase, and superheated refrigerant zones. Log mean temperature difference (LMTD) method has been used in each zone for the heat transfer modeling.

For given mass flow rate, an important parameter, air mass velocity has been evaluated by,

$$G_a = \frac{\dot{m}_a}{A_{fr}} \tag{4.6}$$

The heat transfer coefficient of the air over the condenser has been calculated by,

$$h_a = \frac{j_a G_a c_{p,a}}{\mathrm{Pr}_a^{2/3}} \tag{4.7}$$

The Colburn factor correlation for the wavy fin is given by (Jungi et al., 2007),

$$j_a = 0.836\ (R_{ea})^{-0.2309} \left(\frac{F_p}{F_h}\right)^{0.1284} \left(\frac{F_p}{2A}\right)^{-0.153} \left(\frac{L_d}{L_f}\right)^{-0.236} \tag{4.8}$$

The overall efficiency of the fin has been determined by,

$$\eta_o = 1 - \frac{A_f}{A_o}\left(1 - \eta_f\right) \tag{4.9}$$

The fin efficiency of a wavy fin has been predicted by using the approximation method as described (Schmidt, 1949). Nusselt number of refrigerants in both sub-cooled and superheated zones has been evaluated by,

$$Nu_r = 0.023\left(\mathrm{Re}_r\right)^{0.8}\left(\mathrm{Pr}_r\right)^n \tag{4.10}$$

Where n=0.4 for heating and n=0.3 for cooling.

Nusselt number of the refrigerant in the two-phase region has been obtained by (Wang et al., 2002),

$$Nu_r = 0.027\,\mathrm{Pr}_l(\mathrm{Re}_l)^{0.6792}\,x^{0.02208}\left[\frac{1.376 + 8\left(X_{tt}\right)^{0.5}}{\left(X_{tt}\right)^2}\right] \tag{4.11}$$

Where, $X_{tt} = \left(\mu_l / \mu_v\right)^{0.1}\left((1-x)/x\right)^{0.9}\left(v_l / v_v\right)^{0.5}$

For each zone, the overall heat transfer coefficient based on the air-side area has been calculated by,

$$\frac{1}{(UA)_o} = \frac{1}{\eta_o h_a A_o} + \frac{1}{h_{ri} A_i} \tag{4.12}$$

Then, the heat transfer in each zone has been obtained by,

$$\mathrm{Q}_{cond} = (UA)_o (LMTD) \tag{4.13}$$

Total heat transfer in the cross-flow wavy fin condenser from the refrigerant to air has been calculated by adding the heat transfer in superheated, two-phase, and sub-cooled zones.

4.1.3. Evaporator model

The evaporator model is slightly complicated due to both heat and mass transfers. Here, the evaporator is considered a wavy fin and tube cross-flow type heat exchanger. As shown in Fig. 4, the flow length is divided into three zones: (i) Zone-1: sensible cooling of air and superheating of refrigerant, (ii) Zone-2: sensible cooling of air and evaporation of the refrigerant, and (iii) Zone-3: cooling and dehumidification of air and evaporation of refrigerant. Calculation of heat transfer coefficient of air for all zones and that for superheated refrigerant are the same as in the condenser model.

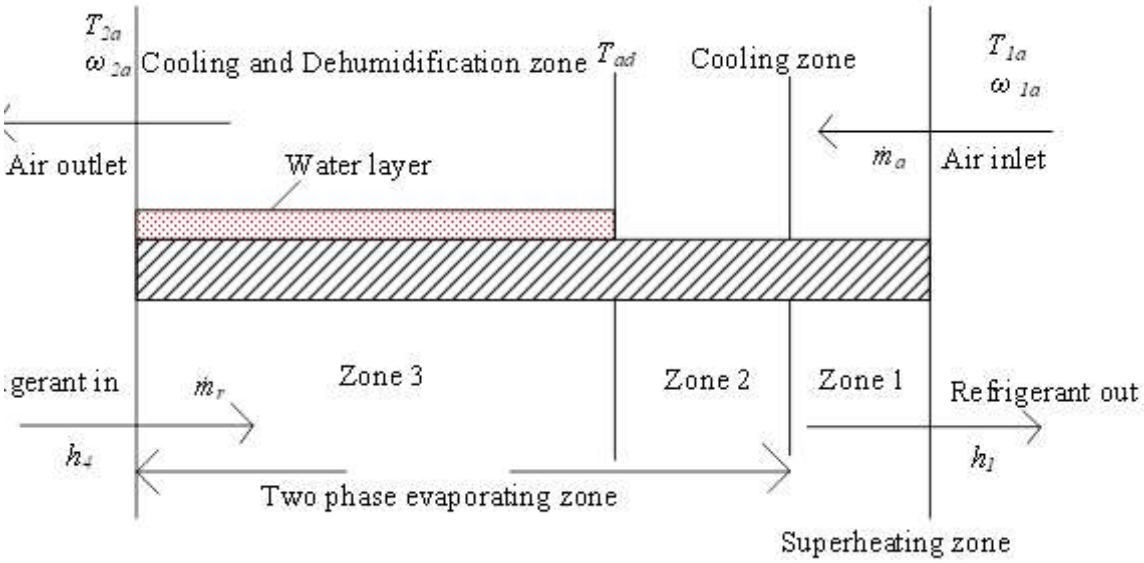

Fig. 4.4. Various heat transfer zone in the evaporator

The heat transfer coefficient for the evaporating zone has been calculated by (Kenning and Cooper, 1989),

$$h_r = \left(1 + 1.8 X_{tt}^{-0.87}\right) h_l \tag{4.14}$$

Where, $h_l = 0.023\left(\mathrm{Re}_l\right)^{0.8}\left(\mathrm{Pr}_l\right)^{0.4}\left(k_l / D\right)$

Eqs. 4.12-4.13 are applicable for the heat transfer calculation for zones 1 and 2. But in zone 3, there will be an extra resistance due to the layer of water over the tubes and extra heat transfer due to condensation of water vapor. At the water layer, the inner

side overall heat transfer coefficient of air with refrigerant evaporating (zone 3) is given by,

$$\frac{1}{(UA)_i} = \frac{1}{h_{ri} A_i} + \frac{w}{k_w A_o} \tag{4.15}$$

Where w = thickness of the water layer on the wet zone.

The outer side overall heat transfer coefficient is presented by,

$$(UA)_o = \eta_o h_a A_o \tag{4.16}$$

And the total heat transfer that takes place in the wet region is calculated by,

$$Q_{evap} = (UA)_o (LMTD) + \dot{m}_a h_{fg} \left(\omega_{1a} - \omega_{2a} \right) \tag{4.17}$$

The total heat transfer in the evaporator is calculated by adding the heat transfer in superheated (zone 1), two-phase zone with cooling (zone 2), and two-phase zone with cooling and dehumidification (zone 3).

From the mass balance equation, using the Lewis correlation and replacing the mass transfer coefficient, the humidity ratio of the air at the exit to the evaporator is given by,

$$\dot{m}_a \left(\omega_{1a} - \omega_{2a} \right) = \eta_o h_m A_o \left(\omega_{1a} - \omega_{as} \right) \tag{4.18}$$

$$\omega_{2a} = \omega_{1a} - \frac{2}{1 + 2\dot{m}_a c_{pam} / (UA)_o} \left(\omega_{1a} - \omega_{as} \right) \tag{4.19}$$

Where, h_m is the mass transfer coefficient, evaluated by using Lewis correlation, and [[

ω_{as} is the saturated humidity ratio of air corresponding to the mean water surface (evaporator tube) temperature (T_w), which is given by,

$$T_{w,evap} = \frac{Q_{evap}}{(UA)_i} + T_r \tag{4.20}$$

4.1.4. Capillary tube model

The expansion process in the capillary tube has been assumed to be isenthalpic. The pressure drop takes place inside the capillary tube due to the friction inside the tube as well as due to an increase in the velocity of the refrigerant flow from higher condenser pressure to the lower evaporator pressure.

$$h_3 = h_4 \tag{4.21}$$

4.1.5. Fan model

In the HPD system, the fan is used to develop a pressure difference sufficient to maintain the required airflow rate in the system. Neglecting the air pressure drop in the connecting ducts, the total air pressure drop in the HPD has been calculated by,

$$\Delta p_a = \Delta p_{evap} + \Delta p_{cond} + \Delta p_{dryer} \tag{4.22}$$

Where, $\Delta p = G_a^{\,2} f_a \left(A_o / A_c\right) / \left(2\rho_a\right)$

Where, f_a is a friction factor for dry air and calculated by (Turaga et al., 1988),

$$f_a = 0.589\left(A_o / A_p\right)^{-0.28}\left(R_{ea}\right)^{-0.27} \tag{4.23}$$

$$R_{ea} = G_a\left(4A_cL / A_o\right) / \mu_a$$

The friction factor for pressure drop in the wet region has been calculated by (Turaga et al., 1988),

$$f_w = 0.318 f_a^{-0.04}\left(s_f / T_f\right)^{0.4} R_{ea}^{-0.42} \tag{4.24}$$

Then the fan power has been calculated by,

$$\mathrm{W_{fan}} = \dot{m}_a \Delta p_a / \left(\eta_{fan}\rho_a\right) \tag{4.25}$$

4.1.6. Dryer model

The heat and the mass transfer phenomena in the batch type dryer depend on air inlet condition, flow rate, flow direction, and nature of drying material. The drying kinetics of the material is strongly dependent on the properties of the products being

dried. So it is difficult to predict the behavior of the heat and mass transfer in the dryer due to the many restrictions. The air inside the drying chamber in the flow direction is assumed to follow the constant wet-bulb temperature in the psychrometric chart. In this study, the dryer is treated as fully insulated, and no heat transfer between the dryer and the surroundings. In this theoretical study, the carrot is considered as the drying material and the drying kinetics of the carrot are used for the calculation of moisture removal rate, moisture content and specific moisture extraction rate (SMER), and the moisture ratio (MR) given by Midilli thin-layer drying model (Sonmete et al., 2017). Hence, the moisture content of exit air is given by,

$$\mathrm{MR}=\frac{(M_o - M_e)}{(M_i - M_e)} = a * \exp\left(-K_p {t_d}^n\right) + b\, t_d \tag{4.26}$$

Where M_e is the equilibrium moisture content of the material in the drying which depends on the material, drying air temperature, and the relative humidity. The equilibrium moisture content of the modified Henderson model (Khakhanmalee et al., 2008) is given by the following,

$$\mathrm{M_e}=\left[\frac{-\ln(1-\mathrm{RH_{3a}})}{0.00013*(T_{3a}+74.481)}\right]^{\left(\frac{1}{1.3339}\right)} \tag{4.27}$$

Where drying constants for carrot have been evaluated by (Sonmete et al., 2017),

$$a = 1.02 - 0.026\ln(V_a)$$

$$K_p = -4.949 + 1.433\ln(T_{3a})$$

$$n = 0.853\exp(0.856 / T_{3a})$$

$$b = 0.004\exp(0.379 / V_a)$$

Using mass balance between the drying air flowing through the dryer and the drying material, the specific humidity of air at the dryer outlet has been obtained by,

$$\omega_{5a} = \frac{m_p \left(Mi - Mo\right)}{t_d \dot{m}_a} + \omega_{4a} \tag{4.28}$$

Air temperature exit to the drying chamber has been calculated by,

$$T_{5a} = \frac{T_{4a}\left(c_{pa} + \omega_{4a} c_{pv}\right) + h_{fg}\left(\omega_{4a} - \omega_{5a}\right)}{\left(c_{pa} + \omega_{5a} c_{pv}\right)} \tag{4.29}$$

The drying efficiency of the heat pump dryer is a very important performance parameter, which indicates, how efficient the dryer is working and has been evaluated by,

$$\mathrm{DE} = \frac{\left(\omega_{5a} - \omega_{4a}\right)}{\left(\omega_{sat} - \omega_{4a}\right)} = \frac{\left(T_{4a} - T_{5a}\right)}{\left(T_{4a} - T_{sat}\right)} \tag{4.30}$$

The energetic performance parameters are calculated based on the equations as discussed in Chapter 3. The exergy in both refrigerant and air has been obtained by neglecting the kinetic and potential energies of the fluid as well as neglecting the changes in the chemical composition, which is expressed as discussed in Chapter 3.

4.1.7. Simulation and validation

A simulation code has been developed in Engineering Equation Solver (EES) platform based on the above mathematical model. The inputs are as follows: initial moisture content of carrot slices, air volume flow rate, inlet air temperature, and specific humidity, component specifications, evaporator, and condenser saturation temperatures. The calculation steps are as follows: with the guess value of refrigerant superheat (T_1) and the evaporator pressure (P_1), all the states points are calculated using compressor, evaporator, and condenser models, and the exact value of T_1 has been calculated by Newton-Raphson iteration method based on Eq.4.21 (Capillary tube model). The flow chart for the entire simulation is given in Fig. 4.5. Then, the humidity ratio and the temperature of the air at the inlet and exit to the drying chamber have been calculated

based on heater and dryer models. Finally, the different performance parameters of the heat pump dryer have been calculated.

For the validation of the simulation results, open type experimental setup of a heat pump dryer was designed and developed. The developed experimental setup is shown in Fig. 3.2, and the different component of the system is indicated in the HPD system. The specification of the different components of the heat pump dryer is considered for the validation of the simulation result is provided in Table 3.1. For the validation of the simulation model, the same air input conditions, mass flow to the evaporator rate, and the drying material (carrot) in the dryer have been considered. The drying air temperature was measured at the inlet and outlet of the drying chamber, evaporator, and condenser. The total energy consumption for the compressor and the fan was measured by the energy meter. The temperature and the pressure on the refrigerant side are measured by the thermocouple and the pressure gauge at a different positions in the cycle. Hygrometers and thermocouples were used for measuring the evaporator and dryer inlet and outlet air's relative humidity and temperature. The performance parameters considered for the validation are moisture extraction rate (MER), specific moisture extraction rate (SMER) and coefficient of performance(COP), and specific energy consumption (SEC), which are given in Table 4.2. The deviations of the simulation result with experimental for MER, SMER and COP are 5.87%, 19.5%, and 11.3% respectively, which are justifiable.

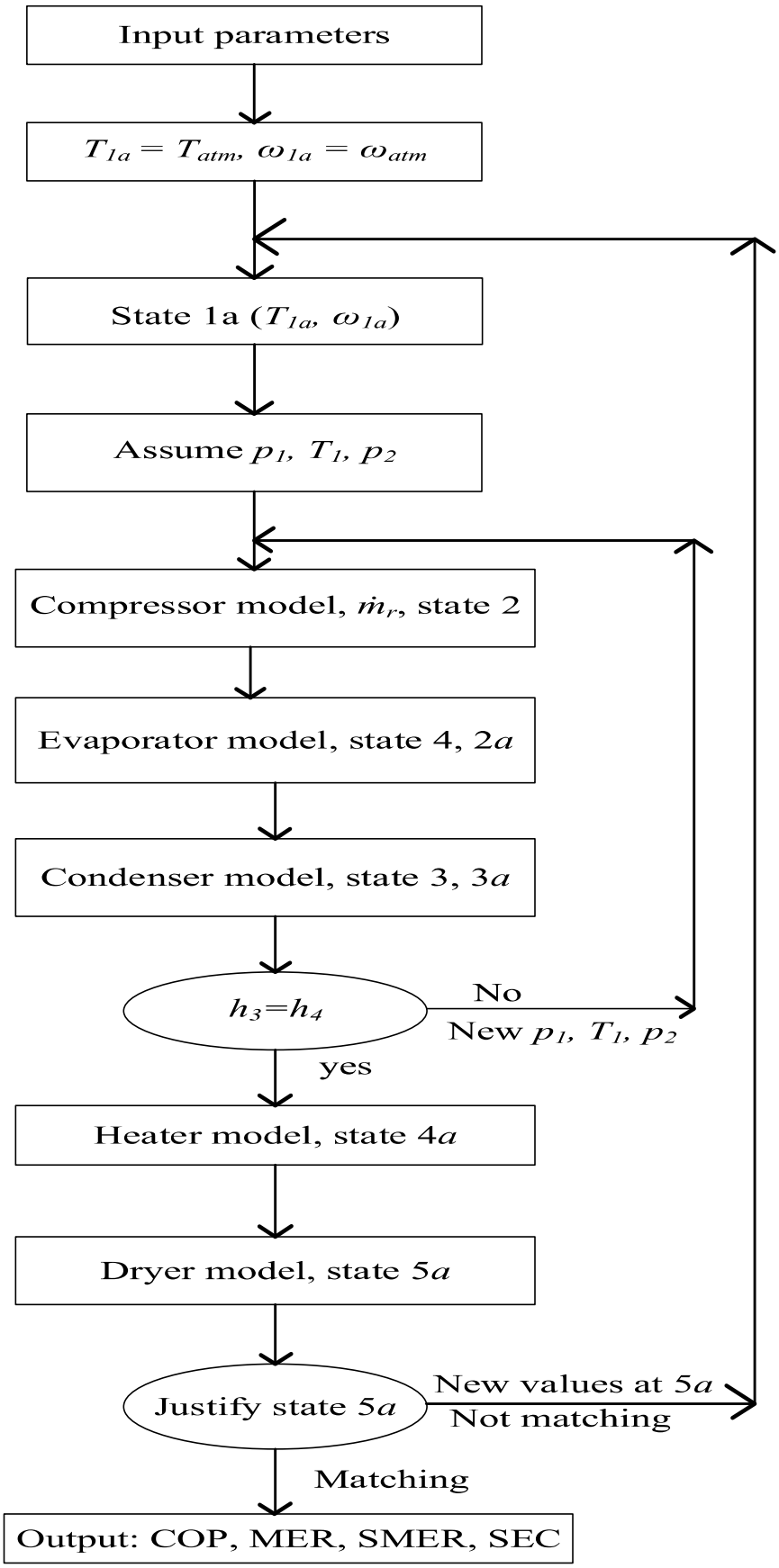

Fig. 4.5. Flow chart of the overall simulation

Table: 4.2. Validation of the simulation result with experimental data

Performance parameter	Simulation result	Experimental result
Air velocity (m/s)	1.0	1.0
Atmospheric air temperature °C)	30	30
Atmospheric air relative humidity (%)	70.6	70.6
MER (kg/h)	0.3931	0.37
SMER (kg/kWh)	1.069	0.86046
COP	4.318	3.83
SEC (kWh/kg)	0.7878	1.1621

4.2 Results and discussion

The performance of the HPD is mainly affected by the drying time and the energy consumption because the increase in drying time causes an increase in power input and a decrease in moisture removal rate from the products. Hence, the variation of various performance parameters such as MER, SMER, drying efficiency, moisture content, and dryer outlet temperature with drying time are studied for the inlet condition of drying air as T_{1a}=28°C and RH_{1a}=76%. The material considered in this analysis is 7 kg of carrot with an initial moisture content of 86% (wet basis). The temperature, humidity ratio, and the velocity of the air at the inlet are 28°C, 0.019 g/g, and 2 m/s, respectively. The specifications of the different components of the heat pump drying system used in the simulation are given in Table 3.1. A comparison of various performance parameters for the heat pump-based dryers is shown in Table 4.3 with the same amount of total power input (2 kW) to the system. Results are shown for the final moisture content of carrot of 12% (wet basis). As shown, heat pump-based drying is superior to hot air drying in terms of all performance parameters.

Table: 4.3. Performance comparison HPD for different refrigerants

Performance parameters	R134a HPD	R290 HPD	R152a HPD	R1234yf HPD	R600a HPD	R32 HPD	R1234ze(E) HPD	R600 HPD
Evaporator outlet temperature (°C)	23.54	23.56	23.65	23.58	23.57	23.4	23.86	23.5
Evaporator outlet humidity ratio	.01848	.0185	.01859	.01853	.01851	.018	.01889	.018
Dryer inlet temperature (°C)	37.32	37.63	37	37.45	38.74	38.9	36.71	37.3
Volumetric heating capacity (MJ/m^3)	8.39	7.358	7.474	8.3031	7.326	8.59	7.135	7.62
COP_{hp}	6.212	4.833	6.386	6.189	4.65	3.18	6.827	4.81
COP_{ws}	1.677	1.666	1.639	1.662	1.689	1.73	1.566	1.68
MER (kg/h)	1.022	1.054	1.061	1.011	1.096	1.11	0.9426	1.02
SMER (kg/kWh)	0.511	0.507	0.557	0.5057	0.5296	0.53	0.4712	0.51

Drying time (h)	5.068	5.11	4.66	5.121	4.977	4.88	5.469	5.06
SEC (kWh/kg)	1.957	1.93	1.799	1.977	1.882	1.88	2.122	1.95
DE	0.2644	0.264	0.2974	0.2665	0.2707	0.26	0.2593	0.26

Fig. 4.6 illustrates the variation of the dryer outlet air temperature with the drying time. As shown, initially the dryer outlet temperature decreases sharply with time due to the more heat transfer between the product and the drying air but after some time as the temperature of the product increases, the heat transfers rate decreases and the dryer outlet temperature starts to increase slowly. The maximum air outlet temperature of the dryer is R32 and the minimum for R1234ze(E) due to the highest and lowest dryer inlet temperature. The air outlet temperature of the dryer for R134a, R290, R152a, R600a, R1234yf, and R600 are in between the R1234ze(E) and R32. Variation of dryer outlet relative humidity (depends on the dryer outlet temperature and the specific humidity of the air) with drying time is shown in Fig. 4.7. As the dryer outlet temperature first decreases with time and hence the relative humidity increases but after some time, the temperature starts to increase. Also, the relative humidity of air starts to decrease with time because there is very less increase in specific humidity of air due decrease in moisture removal rate from the drying material. As shown in the figure, the dryer outlet air relative humidity is maximum for R1234ze (E) due to the lower moisture removal rate from the drying product. Whereas, dryer outlet air relative humidity is minimum for the R32 due to the higher removal rate from the product.

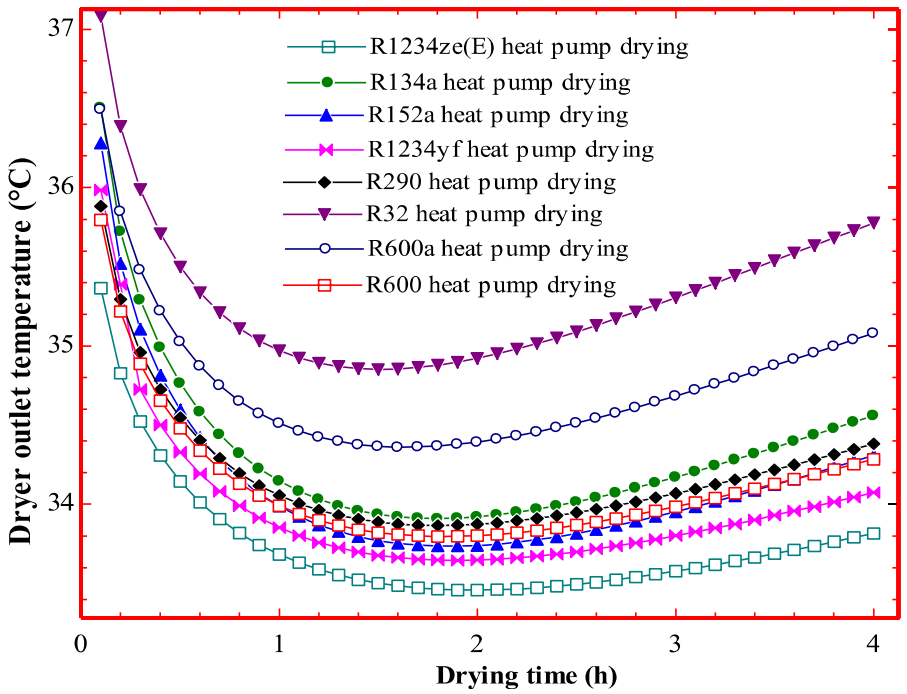

Fig. 4.6. Variation of dryer outlet temperature with drying time

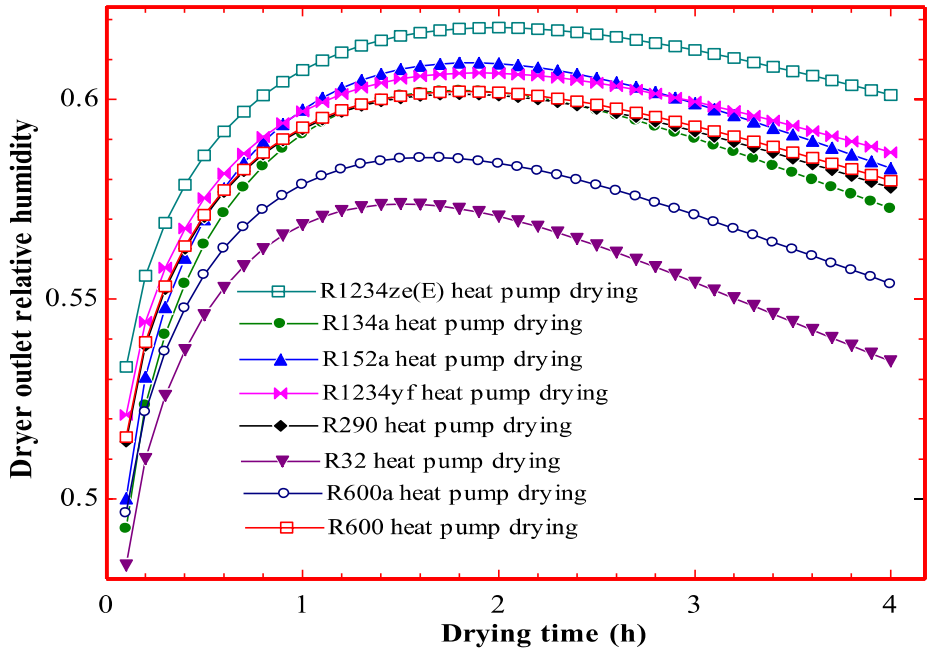

Fig. 4.7. Variation of dryer outlet relative humidity with drying time

Fig. 4.8 shows the variation in the moisture ratio with the drying time for HPD for different refrigerants. As shown, the moisture ratio decreases from the initial value of 0.99 to the final value of 0.12 with drying time due to the moisture removal from the product by air passing through the drying chamber. The moisture content and the

moisture ratio decrease exponentially from the initial to the final value. For heat pump dryer using R32, it decreases more sharply than using other refrigerants due to getting higher condenser outlet temperature of air for the same energy consumption and removing moisture at a faster rate. Values of moisture ratio change are nearly close for the HPD using R135a. R600a, R290, R152a, R1234ze(E), and R600 due to nearly the same condenser outlet temperature.

As shown in Fig. 4.9, the moisture extraction rate first increases with drying time but after some time it starts decreasing due to the decrease in the amount of moisture content of the product in the drying chamber. When the moisture content of the product is high, the moisture removal rate is also high but as the moisture content of the product decreases, the amount of moisture removed from the product decreases and so MER decreases. The maximum moisture extraction rate is 1.111 (kg/h) for the R32 heat pump drying due to higher drying temperature for the same amount of total power input (heater + fan + compressor) and minimum for the R1234ze(E). The average moisture extraction rate for R134a HPD, R290, R152a, R600a, R1234yf, R32, R1234ze(E) and R600 HPD are 1.022, 1.054, 1.061, 1.011, 1.096, 1.111, 09426 and 1.023kg/h, respectively.

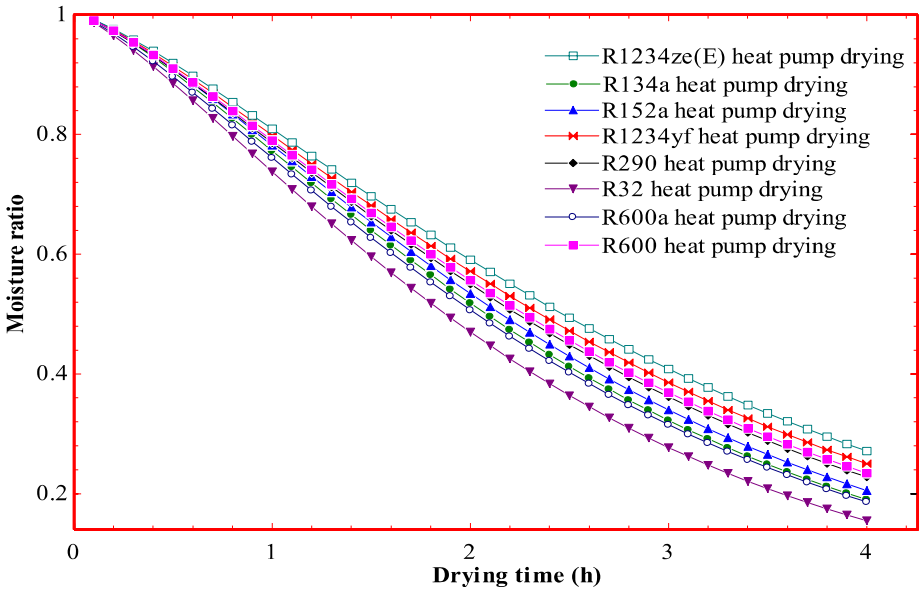

Fig. 4.8. Variation of moisture ratio with drying time

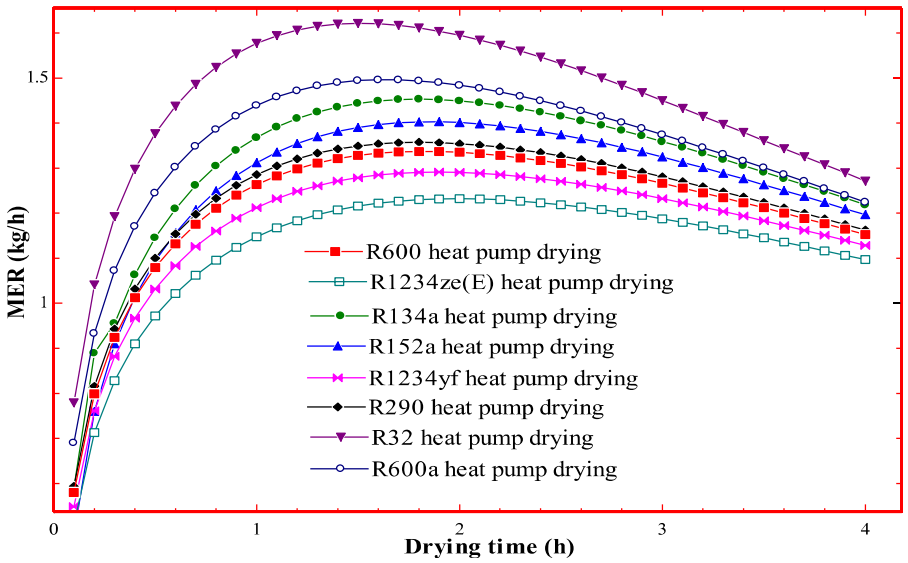

Fig. 4.9. Comparison of change in MER with drying time

Variation of specific moisture extraction rate (SMER) with drying time is shown in Fig. 4.10, which follows the same trend as moisture extraction rate for the HPD because the MER and SMER both depend on the amount of moisture removes from the product. It can be concluded that the SMER has the highest value for R152a and the lowest value for the R1234ze(E) heat pump drying. The specific moisture extraction rate is maximum for R152a because of less drying time required. The average values of SMER for R134a, R290, R152a, R600a, R1234yf, R32, R1234ze(E) and R600 are 0.511, 0.507, 0.557, 0.506, 0.530, 0.530, 0.4712 and 0.5117kg/kWh, respectively.

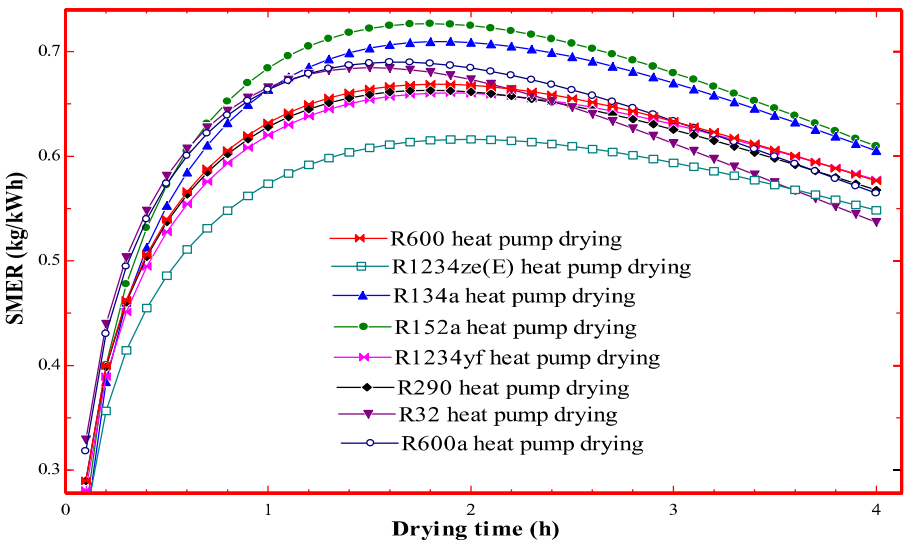

Fig. 4.10. Variation of SMER with drying time

The variation in moisture extraction rate with the moisture content of the drying material is shown in Fig. 4.11. As shown, the moisture extraction rate first increases with moisture content, but after a certain range of moisture content, it starts to decrease. Initially, the air removes less amount of moisture from the product when the moisture content is high due to the start of the establishment of heat and mass transfer between drying air and material, so the moisture extraction rate is low.

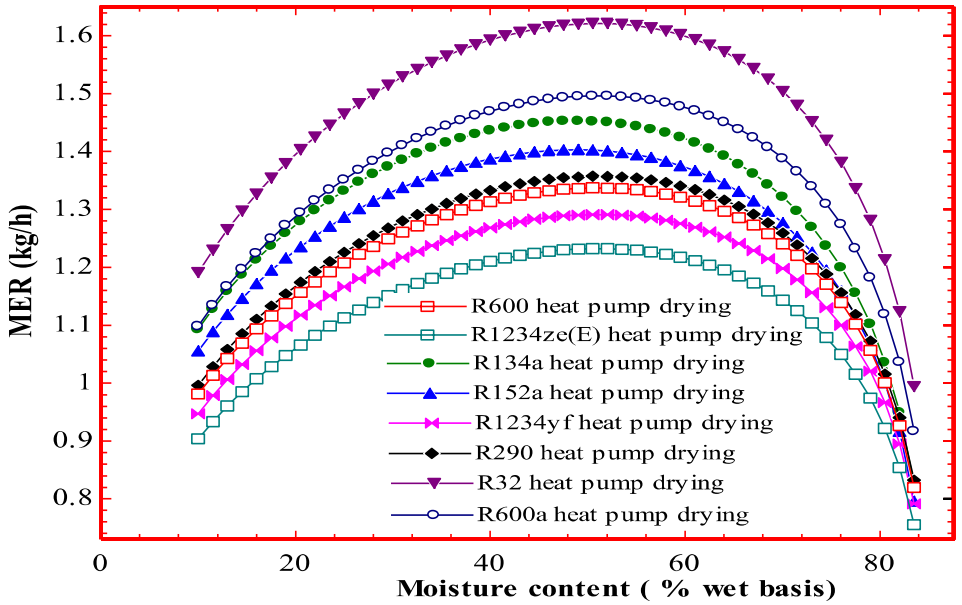

Fig. 4.11. Variation of moisture extraction rate with material moisture content

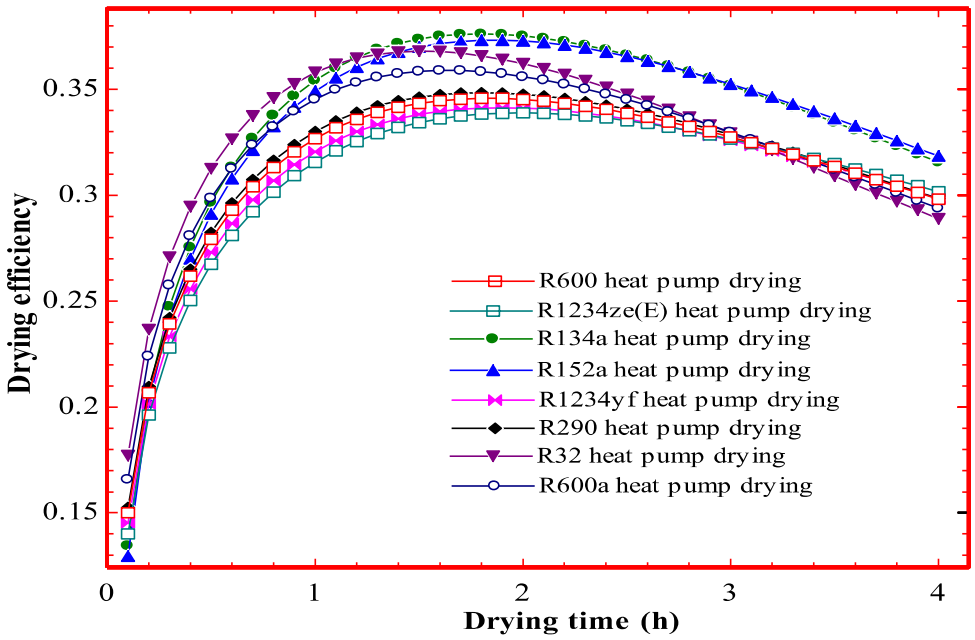

Fig. 4.12. Variation of drying efficiency of HPD with drying time

But at lower moisture content, the MER is low due to a decrease in diffusivity of moisture from the material. The MER is maximum for the R32 followed by R600a and minimum for R1234ze(E).

The variation of drying efficiency with the drying time is shown in Fig. 4.12 for considered refrigerants. The dryer efficiency depends on the dryer outlet temperature and the saturation temperature of the drying air inlet to the dryer. Hence, as shown in the figure, the dryer efficiency first increases as the dryer outlet air temperature decreases but after some time the dryer efficiency starts to decrease due to increases in dryer outlet temperature. The drying efficiency of the heat pump dryer is maximum for R152a.

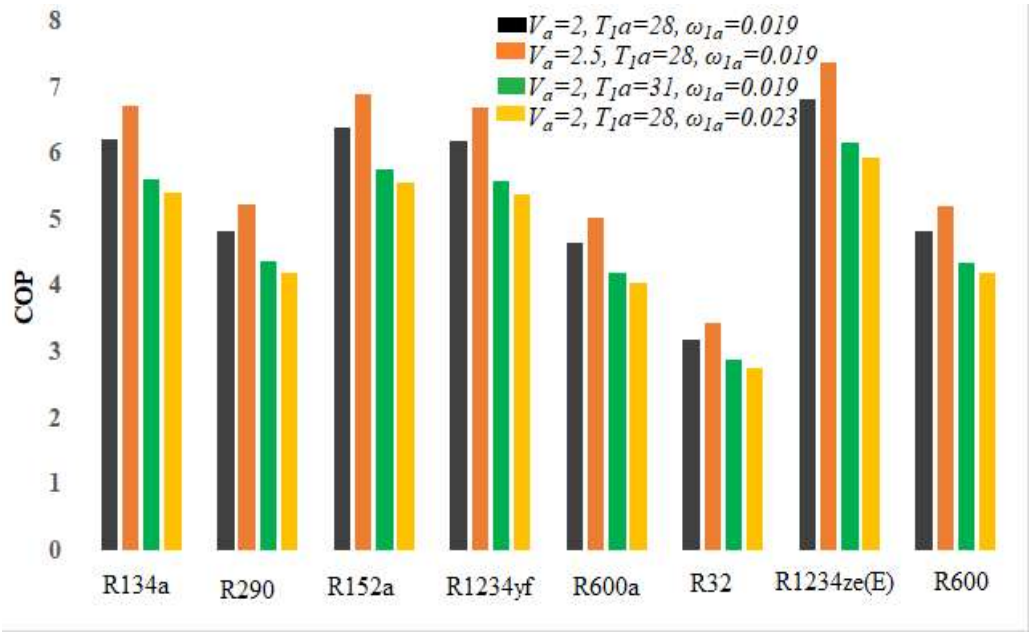

Fig. 4.13. COP of different refrigerants at different atmospheric conditions

Figs. 4.13 and 4.14 show the bar diagram of the COP and the SMER, respectively, for various refrigerants at different atmospheric conditions (inlet to the evaporator). From the figure, it can be seen that the COP of the heat pump drying system increases with an increase in the air velocity but it decreases with an increase in both air inlet temperature and the inlet humidity ratio to the evaporator. The COP decreases with air inlet temperature and humidity ratio due to the increase in the superheat of the refrigerant at

the evaporator outlet and a decrease in the sub-cool of the refrigerant at the condenser outlet. The SMER of the drying system decreases with an increase in the air velocity due decrease in the condenser outlet temperature at a higher velocity and the SMER increases with the increase in the air inlet temperature and the humidity ratio because of an increase in the drying temperature. The drying temperature increases with humidity ratio due increase in the dew point temperature at a higher humidity ratio and evaporator outlet temperature increases finally.

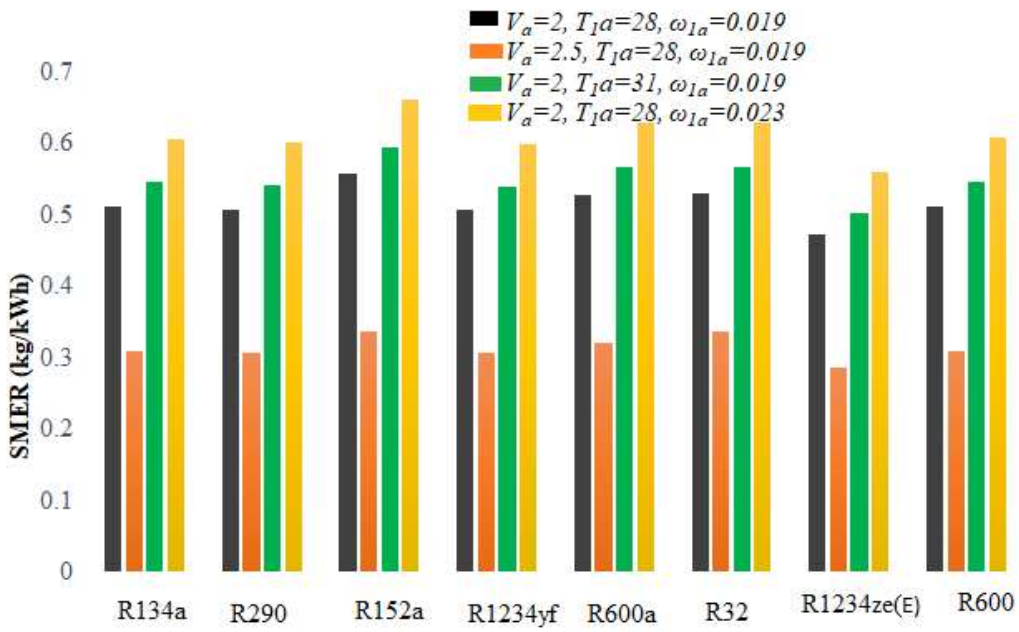

Fig. 4.14. SMER of different refrigerants at different atmospheric conditions

Table 4.4 shows the irreversibility and exergy efficiency of each component in a heat pump drying system using different refrigerants. The irreversibility is maximum in the heat pump dryer using the refrigerant R32 because of the higher temperature at the condenser, higher energy consumption in the compressor, and higher condensation of moisture in the evaporator. The exergy destruction is nearly the same for the refrigerant R134a and R1234yf. The evaporator contributes to maximum exergy destruction due to the condensation of the moisture. Fig. 4.15 shows the total exergy destruction in the

components of HPD using different refrigerants. As shown, total exergy destruction is maximum for R32 (0.7133 kW) and minimum for R1234ze(E) (0.2444 kW). This is due to the higher exergy destruction in the evaporator for R32 than others. R134a and R1234yf are having nearly the same total exergy destruction in the drying system.

Table: 4.4. Irreversibility (W) and exergy efficiency of HPD components

Refrigerant	compressor		condenser		Evaporator		Capillary tube		Dryer		Heater	
	Ex_{dest}	η_{ex}	Ex_{dest}	η_{ex}	Ex_{dest}	η_{ex}	Ex_{dest}	η_{ex}	Ex_{dest}	η_{ex}	Ex_{dest}	η_{ex}
R134a	52.8	0.89	80.6	0.82	95.7	0.71	26.1	0.93	19.1	0.55	38.2	0.022
R290	65.8	0.93	86.0	0.90	91.8	0.85	29.7	0.86	18.8	0.55	36.8	0.0223
R600	67.86	0.92	95.48	0.87	95.9	0.83	19.6	0.86	19.1	0.55	37.16	0.0257
R600a	86.3	0.92	147.2	0.91	96.7	0.90	27.2	0.83	20.1	0.54	33.61	0.0245
R152a	47.8	0.89	78.9	0.80	91.5	0.68	16.1	0.95	18.2	0.55	37.3	0.0211
R32	120.7	0.94	157.1	0.91	99.8	0.93	28.1	0.83	20.3	0.55	33.29	0.0254
R1234yf	52.2	0.90	75.1	0.84	92.3	0.75	32.3	0.92	18.7	0.55	23.79	0.0216
R1234ze(E)	41.3	0.87	61.41	0.79	79.3	0.63	10.6	0.95	16.6	0.56	35.34	0.0207

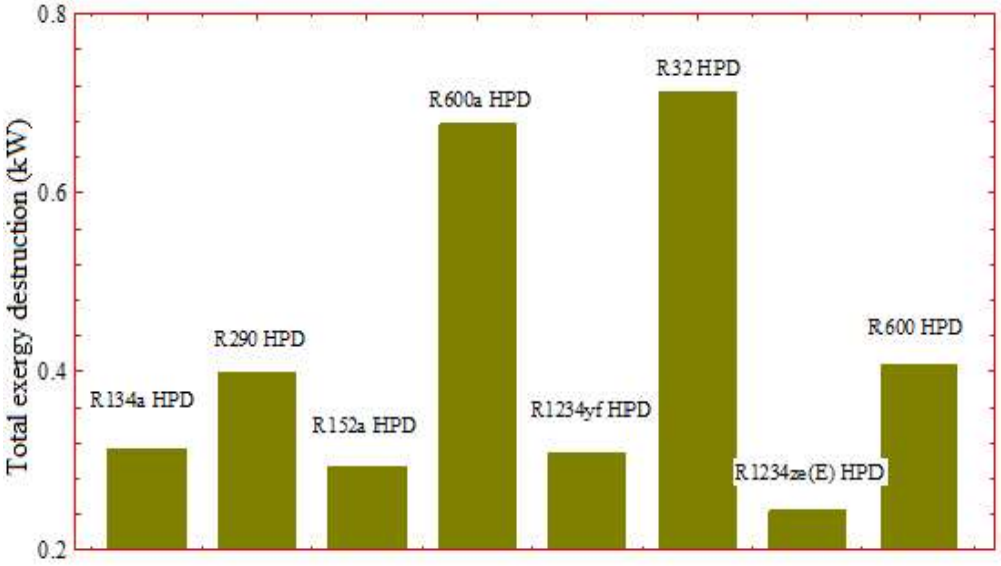

Fig. 4.15. Comparison of total exergy destruction with different refrigerants

4.3 Highlights

The simulation of the batch-type open cycle heat pump dryer has been carried out to predict the energy and exergy performances of the system and compare it with an electric heater-based conventional hot air dryer. Various low-GWP refrigerants have been proposed and compared based on different performance parameters of HPD for carrot drying. The highlights of the study are given below.

- The coefficient of performance of the heat pump (COP_{hp}) and coefficient of performance of the whole system (COP_{ws}) is maximum for R1234zez(E) and R32 respectively, and the (COP_{hp}) minimum for R32.
- The drying efficiency is better for the R152a HPD for the same power input and the average value is 29.74%.
- The moisture extraction rate (MER) is maximum for the R32 (average MER for R32 is about 8.7% more than that for R134a).
- The specific moisture extraction rate (SMER) is maximum for refrigerant R152a (average SMER for R152a is about 9% more than that for R134a).

- The specific energy consumption (SEC) and total drying time are minimum for the R152a HPD and values are 1.79kWh/kg and 4.66h, respectively.
- Total exergy destruction of the heat pump dryer is minimum for R1234ze(E) (0.2444kW) and maximum for R32 (0.713kW) for the same total power input.
- The COP of the system is higher for the higher mass flow rate and lower atmospheric inlet temperature and humidity to the system.
- Within studied refrigerants, R152a and R32 yield better performance; however, R152a may be more favorable for HPD due to lower GWP.